

# **SARS-CoV-2 induces activation and diversification of human plasmacytoid pre-dendritic cells**

Fanny Onodi<sup>1</sup>, Lucie Bonnet-Madin<sup>2</sup>, Léa Karpf<sup>1</sup>, Laurent Meertens<sup>2</sup>, Justine Poirot<sup>1</sup>, Jérôme Legoff<sup>1, 3</sup>, Constance Delaugerre<sup>2, 3</sup>, Ali Amara<sup>2, #</sup> and Vassili Soumelis<sup>1, 4, #</sup>

<sup>1</sup> Université de Paris, Institut de Recherche Saint-Louis, INSERM U976, Hôpital Saint-Louis, 75010 Paris, France

<sup>2</sup> Université de Paris, Institut de Recherche Saint-Louis, INSERM U944 CNRS 7212, Hôpital Saint-Louis, 75010 Paris, France

<sup>3</sup> Laboratoire de Virologie, Hôpital Saint-Louis, APHP, 75010 Paris, France

<sup>4</sup> Assistance Publique-Hôpitaux de Paris (AP-HP), Hôpital Saint-Louis, Laboratoire d'Immunologie, F-75010, Paris, France

# Corresponding authors: [vassili.soumelis@aphp.fr](mailto:vassili.soumelis@aphp.fr); [ali.amara@inserm.fr](mailto:ali.amara@inserm.fr)

## Abstract

Several studies have analyzed antiviral immune pathways in severe COVID-19 patients. However, the initial steps of antiviral immunity are not known. Here, we have studied the interaction of isolated primary SARS-CoV-2 viral strains with human plasmacytoid pre-dendritic cells (pDC), a key player in antiviral immunity. We show that pDC are not permissive to SARS-CoV-2 infection. However, they efficiently diversified into activated P1-, P2-, and P3-pDC effector subsets in response to viral stimulation. They expressed checkpoint molecules at levels similar to influenza virus-induced activation. They rapidly produced high levels of interferon- $\alpha$ , interferon- $\lambda$ 1, IL-6, IP-10, and IL-8. Importantly, all major aspects of SARS-CoV-2-induced pDC activation were inhibited by hydroxychloroquine, including P2- and P3-pDC differentiation, the expression of maturation markers, and the production of interferon- $\alpha$  and inflammatory cytokines. Our results indicate that pDC may represent a major player in the first line of defense against SARS-CoV-2 infection, and call for caution in the use of hydroxychloroquine in the early treatment of the disease.

## Introduction

Severe Acute Respiratory Syndrome-Coronavirus-2 (SARS-CoV-2) is the third zoonotic coronavirus that emerged in the last two decades. SARS-CoV-2 is the causative agent of coronavirus disease 2019 (COVID-19) that appeared in late 2019 in Wuhan, Hubei province in China (Nandakumar, 2020; Sheahan and Frieman, 2020). SARS-CoV-2 became rapidly pandemic, and infection have now been detected in 216 countries and territories, and is responsible for approximately 10 million confirmed cases and 500,000 deaths as of 26 of June 2020 (WHO weekly update).

- SARS-CoV-2 infection may lead to a diversity of clinical presentations, ranging from asymptomatic or mild “flu-like” syndrome, to severe and life-threatening acute respiratory failure. Disease aggravation usually occurs after 8 to 10 days following initial symptoms (Tang et al., 2020). At this late stage, three main factors were shown to contribute to the progression and severity of the infection (Tang et al., 2020): 1) viral persistence was evidenced in the lung and systemic circulation, although it is not constant (Tang et al., 2020), 2) an excess production of pro-inflammatory cytokines, such as IL-1b and IL-6 (Tay et al., 2020; Arnaldez et al., 2020), 3) a defect in type I interferon (IFN) production, especially in critically ill patients (Tay et al., 2020; Acharya et al., 2020). Although these abnormalities were confirmed in several studies, their origin and underlying mechanisms remain mostly unknown. In particular, it is not known whether an imbalance between inflammatory cytokines and type I IFN occurs early in the disease, at the stage of the primary infection, and whether the virus itself may be responsible. To fill this gap of knowledge, it becomes essential to investigate the early innate immune response to SARS-CoV-2. Among the immune cells that are involved in innate anti-viral immunity, plasmacytoid pre-dendritic cells (pDC) play a particularly important role as the major source of type I IFN in response to viral infection (Liu, 2005). PDC can sense a large array of viruses including the coronaviruses murine hepatitis virus (MHV) and the middle east respiratory syndrome coronavirus (MERS) (Scheuplein et al., 2015; Cervantes-Barragan et al., 2007), and respond by producing innate cytokines, including all forms of type I IFNs ( $\alpha$  and  $\beta$ ), type III IFN, and inflammatory cytokines, in particular TNF- $\alpha$  and IL-6 (Liu, 2005; Yin et al., 2012; Gilliet et al., 2008). However, different viruses may induce different cytokine patterns (Thomas et al., 2014), possibly creating an imbalance between IFN versus inflammatory cytokine response.

Additionally, some viruses were shown to subvert pDC functions through different mechanisms not necessarily related to productive infection. This is the case for HIV, which may induce pDC apoptosis in vitro (Meyers et al., 2007) and pDC depletion in vivo (Soumelis et al., 2001; Meera et al., 2010). Human hepatitis C virus can inhibit IFN- $\alpha$  production by pDC through the glycoprotein E2 binding to BDCA-2 (Florentin et al., 2012). Human papillomavirus induces very low IFN response in pDC (Bontkes et al., 2005), which may be due to impaired TLR-7 and -9 signaling (Hirsch et al., 2010). Whether SARS-CoV-2 induces efficient pDC activation, or may interfere with various biological pathways in pDC is currently unknown.

In this study, we have systematically addressed the interactions between clinical SARS-CoV-2 isolates and primary human pDC in order to reproduce the early stages of the infection. We showed that pDC are resistant to productive infection with SARS-CoV-2 strains but still mount substantial IFN responses upon viral challenge. Interestingly, pDC responded to SARS-CoV-2 by a complete activation program, including diversification into effector subsets, production of type I and type III IFN, as well as inflammatory cytokines. We also showed that hydroxychloroquine, an antimalarial drug proposed for treatment of COVID-19 patients (Das et al., 2020; Mahévas et al., 2020), inhibits SARS-CoV-2-induced pDC activation and IFN production in a dose-dependent manner. Our results establish pDC as a potential key player in innate immunity to SARS-CoV-2, and raise caution regarding pharmacological manipulation that could inhibit pDC effector functions.

## Results

### SARS-CoV-2 induces activation and diversification of primary human pDC

In order to efficiently recapitulate SARS-CoV-2-pDC interactions, we used two strains of SARS-CoV-2 primary isolates. Their viral genome sequences were nearly identical with 99.98% identity. Sequence comparison with reference strain Wuhan-Hu-1 (NCBI accession number NC\_045512.2) showed that both strains contain a subset of mutations (C241T; C30307T; A23403G and G25563T), characteristic of the GH clade based on GISAID nomenclature. Human primary pDC were purified from healthy donor peripheral blood mononuclear cells (PBMC) by cell sorting. First, we asked whether SARS-CoV-2 was able to induce pDC activation, and diversification into IFN-producing and/or T cell stimulating effectors, as we previously described for influenza virus A (Flu) (Alculumbre et al., 2018). After 24 hours of culture, SARS-CoV-2-activated pDC efficiently diversified into P1 (PD-L1<sup>+</sup>CD80<sup>-</sup>), P2 (PD-L1<sup>+</sup>CD80<sup>+</sup>), and P3 (PD-L1<sup>+</sup>CD80<sup>+</sup>) pDC subsets, similar to Flu stimulation (Fig 1A). P1-, P2-, and P3-pDC were all significantly induced by SARS-CoV-2 and Flu, as compared to medium control (Fig 1B). In parallel, we observed a sharp decrease in non-activated P0-pDC (PD-L1<sup>-</sup>CD80<sup>-</sup>) (Fig 1A and B). SARS-CoV-2-induced pDC activation was comparable with magnetically- versus FACS-sorted pDC (Fig S1A and S1B), confirming that both methods are suitable for subsequent experiments. All main findings were confirmed on at least three independent experiments using FACS-sorted pDC, with a protocol that excluded AS-DC, a rare dendritic cell (DC) subset that shares some markers and functional features with pDC (Villani et al., 2017), based on CD2, CD5 and AXL expression (Fig S1A).

PDC activation and diversification was observed with two independent primary SARS-CoV-2 strains (Fig 1C), which both induced similar proportions of P1-P3 subsets. PDC diversification was also observed by co-culturing of pDC with SARS-CoV-2-infected Vero E6 cells with a similar efficiency than free SARS-CoV-2 (Fig

S1C). SARS-CoV-2 improved pDC viability as compared to medium condition (Fig 1D), which is compatible with subsequent effector functions.

### **Human pDC are not productively infected by SARS-CoV-2**

Next, we asked whether SARS-CoV-2 -induced pDC activation was dependent on productive infection. We first checked whether pDC express at their cell surface ACE2, the major SARS-CoV-2 entry receptor (Hoffmann et al., 2020, 2). No significant expression was detected using an anti-ACE2-specific antibody, as compared to a low and high expression on Vero E6 and 293T-ACE2 cell lines, respectively (Fig 1E). The ability of pDC to replicate SARS-CoV-2 was then assessed. Human pDC were challenged with SARS-CoV-2 strain 220\_95 at MOI of 2, and cultured for 2h, 24h or 48 h. Our results showed that pDC were refractory to SARS-CoV-2 infection, as evaluated by quantifying 1) the intracellular production of the nucleoprotein antigen (N) (Fig 1F), or the accumulation of viral RNA in SARS-CoV-2-infected cells (Fig S1D), and 2) the release of infectious progeny virus in the supernatants of infected cells using plaque assays (Fig 1G). As positive control, the permissive Vero E6 cells produced high level of the N antigen, increased viral RNA overtime (Fig S1D), and high viral titers following SARS-CoV-2 incubation (Fig 1G). Similar results were obtained with pDC isolated from three independent donors (Fig S1E). Overall, these results show that pDC are resistant to SARS-CoV-2 infection, and are efficiently activated by the virus independently of ACE2 expression. Their viability was not affected by SARS-CoV-2 challenge.

### **Upregulation of major immune checkpoints on SARS-CoV-2-activated pDC**

Activating immune checkpoints play a key role in T cell stimulation, and serve as surrogate markers of DC differentiation (Guermonprez et al., 2002). We first

assessed the dose-dependent effect of SARS-CoV-2 on CD80 expression and subset diversification. CD80 was induced in a dose-dependent manner by SARS-CoV-2 at MOI 0.04 to 1 (Fig 2A). This was accompanied by an increase in P3-pDC subset, and a slight decrease in P1-pDC (Fig 2B). A detailed phenotypic analysis was subsequently performed on pDC after 24 and 48 hours of culture with SARS-CoV-2 (Fig 2C and Fig S2A). Diversification was observed at both time points, with a slight increase in P3-pDC at 48 hours (Fig S2A). P2- and P3-pDC significantly upregulated CD80, CD86, CCR7, and OX40L, as compared to non-activated P0-pDC, in both SARS-CoV-2 and Flu conditions (Fig 2C). PD-L1, and CD62L, an integrin that promotes lymph node homing, were both higher on P1- and P2-pDC (Fig 2C). Expression of checkpoint molecules persisted at 48h, especially the higher CD80 and CD86 expression on P3-pDC (Fig S2B).

### **Efficient production of type I and type III interferons by SARS-CoV-2-activated pDC**

A key and defining function of pDC is their ability to produce large amounts of type I IFN (Gilliet et al., 2008). We measured the production of several cytokines at the protein level after 24 hours of culture. Both SARS-CoV-2 and Flu induced high levels of IFN- $\alpha$ 2 and IFN- $\lambda$ 1, both being critical anti-viral effector cytokines (Fig 3A). IFN- $\alpha$  levels following SARS-CoV-2 activation reached up to 80 ng/ml, indicating a very efficient activation. The chemokine IP-10 was also significantly induced (Fig 3A), possibly due to an autocrine IFN loop (Blackwell and Krieg, 2003). Inflammatory cytokines IL-6 and IL-8 were comparably induced by SARS-CoV-2 and Flu (Fig 3A). However, TNF- $\alpha$  levels were marginally induced by SARS-CoV-2 as compared to Flu activation (Fig 3A). Cytokine production was maintained after 48 hours of viral activation (Fig 3B). Secreted protein levels were similar to 24h levels for most

cytokines. Interestingly, IFN- $\alpha$  levels raised by 3-fold between 24h and 48h for one donor (Fig 3A and B), indicating the possibility of increased production. Such strong IFN producer suggests a potential virus controller.

Because the oropharyngeal mucosa is an entry site for SARS-CoV-2, we aimed at validating our results using pDC purified from tonsils. SARS-CoV-2 induced a marked diversification of tonsillar pDC into all three activated subsets (Fig S2C). Tonsillar pDC efficiently produced IFN and inflammatory cytokines in response to SARS-CoV-2 (Fig S2D). Overall, our results establish SARS-CoV-2 as a very efficient inducer of type I and type III IFN responses. Inflammatory cytokines were induced at similar level than Flu activation, without any significant imbalance that would be suggestive of excessive inflammatory response.

### **SARS-CoV-2-induced pDC activation is inhibited by hydroxychloroquine**

Given that SARS-CoV-2 did not infect pDC, and did not interfere with pDC activation, we asked whether pharmacological agents could modulate pDC diversification and cytokine production. Hydroxychloroquine (HCQ) is known to inhibit endosomal acidification which may diminish pDC activation (Kuznik et al., 2011, 9; Sacre et al., 2012). Additionally, it is being tested in several clinical studies as a potential treatment for COVID-19 (Das et al., 2020; Mahévas et al., 2020). Hence, we addressed its role in SARS-CoV-2-induced pDC activation. Following 24 hours of culture, we found that HCQ inhibited pDC diversification in response to SARS-CoV-2, which is similar to the decrease observed with Flu, used as a positive control (Fig 4A). In particular, P2- and P3-pDC differentiation were almost completely inhibited (Fig 4B). Inhibition of SARS-CoV-2-induced pDC diversification by HCQ was dose-dependent (Fig S3A). The significant decrease in P3-pDC was paralleled by a decrease in CD80, CD86, and CCR7 expression (Fig 4C and D). OX40-ligand



expression was not significantly affected by HCQ (Fig 4C and D). However, HCQ inhibited the appearance of an OX40-ligand<sup>high</sup> pDC population (Fig S3B and S3C), which may impact subsequent T cell activation. Last, we assessed the effect of HCQ on innate pDC functions. We measured cytokine production after 24 hours of SARS-CoV-2-induced pDC activation in the presence or absence of HCQ. We found that IFN- $\alpha$  and  $\lambda$  levels were decreased by HCQ (Fig 4E). This was also the case for IL-6 and IL-8, with a much lesser impact on IP-10 (Fig 4E). Together, these results show that HCQ inhibits SARS-CoV-2-induced pDC diversification and cytokine production.

## Discussion

Type I IFNs are critical cytokines that control viral replication. Several chronic viral infections were associated to poor type I IFN responses (Lee et al., 2013; Snell et al., 2017; Marsili et al., 2012; Dolganiuc et al., 2006). In COVID-19 patients, decreased serum levels of type I IFN were associated with severity in late stage infection, and increased viral load (Tay et al., 2020; Acharya et al., 2020). This raised the question as to whether SARS-CoV-2 was intrinsically capable of inducing a robust IFN response, or on the contrary could interfere with IFN production and other antiviral immune pathways. In this study, we have used primary SARS-CoV-2 isolates and human primary pDC in order to increase the relevance to a naturally occurring infection. Our results demonstrate that SARS-CoV-2 is a strong IFN inducer by efficiently stimulating primary pDC. Viral sensing was independent of the expression of the ACE2 entry receptor or the ability of the virus to replicate in pDC. However, the precise molecular mechanisms involved remain to be investigated. Both type I and type III IFNs were induced at high levels upon SARS-CoV-2 stimulation. This strongly

suggests that the defects observed in critically ill COVID-19 patients are acquired during disease evolution through secondary events, not necessarily associated to direct effect of the virus. Possible mechanisms could be related to inflammatory cytokines, such as TNF, and endogenous glucocorticoid response, both being able to promote pDC apoptosis ((Abe and Thomson, 2006). However, additional mechanisms may be involved and need to be explored in the context of severe COVID-19.

An excessive production of inflammatory cytokines, such as IL-1  $\beta$ , IL-6 and TNF, was associated to COVID-19 severity (Tay et al., 2020; Arnaldez et al., 2020; Vabret et al., 2020). Their cellular source and the underlying mechanisms are currently unknown. Our results indicate that SARS-CoV-2-induced pDC activation promotes a balanced production of innate cytokines, including large amounts of type I and type III INFs, without any significant excess in inflammatory cytokines. This suggests that pDC activation may not be a causal factor of COVID-19 aggravation. In support to that, recent studies indicated that endothelial cells may be a target of SARS-CoV-2 infection, and could be at the origin of the systemic and multi-organ production of inflammatory cytokines (Pons et al., 2020). Bronchial epithelial cells could also be involved in the production of high levels of IL-6, which were not detected in the serum and in PBMC transcriptomic studies in severe COVID-19 (Wilk et al., 2020). This supports the view of pDC as being protective through an early and efficient production of antiviral cytokines, with later defects due to currently unknown mechanisms, associated with late stage aggravation. On the contrary, non-professional innate immune cells such as endothelial cells and bronchial epithelial cells may be involved in the secondary worsening of COVID-19 through the excessive and uncontrolled production of inflammatory cytokines. Several therapeutic

approaches have been explored and are currently being tested in clinical trials on COVID-19 patients (Vabret et al., 2020; Tay et al., 2020). These include antiviral agents (Yang et al., 2020), immune-modulatory molecules, such as glucocorticoids (Fernández Cruz et al., 2020), and anti-inflammatory molecules, such as HCQ (Touret and de Lamballerie, 2020; Lecuit, 2020). This latter drug was additionally shown in *in vitro* studies to interfere with SARS-CoV-2 replication (Wang et al., 2020). The difficulty in designing current and future COVID-19 treatment strategies lies in part in the complexity of the host-virus interactions. Ideally, an efficient therapy should control the excessive and potentially pathogenic inflammatory cytokine response, while preserving antiviral effector pathways in order to efficiently control viral replication. In our study, we have shown that SARS-CoV-2 effectively induced type I IFN production by pDC during initial encounter with the virus. Given the importance of IFN responses in the control of viral infections, pharmacological agents that decrease IFN production should be avoided. Our results showing that HCQ could inhibit all aspects of SARS-CoV-2-induced pDC activation call for a lot of caution in the use of that drug in the context of COVID-19. A favorable cost-benefit ratio would be expected only if a strong direct antiviral effect was demonstrated, associated with an efficient ability to control the production of pathogenic inflammatory cytokines. Else, interfering with pDC anti-viral response could contribute to a less efficient control of SARS-CoV-2 infection and subsequent worsening of the disease. Continued efforts in mapping and dissecting immune effector pathways to SARS-CoV-2 will be of major importance in order to design efficient treatment strategies adapted to each patient and stage of the infection.

## Materials and methods

## **PDC isolation and cell culture**

Buffy coats from healthy human donors were obtained from Etablissement Français du Sang, Paris, Saint-Antoine Crozatier blood bank. Peripheral blood mononuclear cells (PBMCs) were isolated through Ficoll density gradient centrifugation (Ficoll-Paque; GE Healthcare). PDC were isolated through a first step of pDC magnetic sorting (Human Plasmacytoid DC Enrichment Kit; StemCell), and subsequent flow cytometric sorting on the basis of live, lineage<sup>-</sup> (CD16, CD14, CD19, CD20, CD56 and CD3), CD11c<sup>-</sup> CD4<sup>+</sup>, and CD2<sup>-</sup> CD5<sup>-</sup> cells to a 98% purity. Due to some logistic issues, alternatively frozen PBMCs from Etablissement Français du Sang, Paris, Saint Louis blood bank, were thawed and placed at 37°C for 2h for cell recovery. pDC were then magnetically sorted (Human Plasmacytoid DC Enrichment Kit; StemCell). PDC enrichment was assessed based on the cytometric sorting panel, and was ranged from 71 to 90%.

African green monkey kidney epithelial Vero E6 cells (ATCC, CRL-1586) were cultured in Dulbecco's Modified Eagle Medium (DMEM; Thermo Fisher Scientific) supplemented with 10% FBS, 1% penicillin-streptomycin, 1% GlutaMAX and 25 mM Hepes.

## **SARS-CoV-2 primary strain isolation and amplification**

SARS-CoV-2 viruses were isolated from nasopharyngeal swab specimens collected at Service de Virologie (Hospital Saint Louis, Paris). Samples were centrifugated at 4,000 x g for 10 min then filtered using a 0.45 µm filter, and diluted 1:1 with DMEM-4% (DMEM supplemented with 4% FBS, 1% penicillin-streptomycin, 1% GlutaMAX and 25 mM Hepes). Vero E6 cells were seeded in 96-well cell culture plate (15,000 cells/well), and incubated at 37°C with 200µl of inoculum and observed daily for

cytopathogenic effects (CPE) by light microscopy. Substantial CPE were seen at 72-96 hours post inoculation. Culture supernatants were then collected, clarified by centrifugation, filtered using a 0.45 µm filter and kept at -80°C. We confirmed SARS-CoV-2 replication by RT-qPCR and whole viral genome sequences were obtained by next generation sequencing using Illumina MiSeq sequencers. Strains sequences have been deposited in the Global Initiative of Sharing All Influenza Data (GISAID) database with accession ID EPI\_ISL\_469284 (220\_95) and EPI\_ISL\_469283 (211\_61). All viruses belong to the GH clade.

SARS-CoV-2 strains were further propagated on Vero E6 in DMEM-2% (DMEM supplemented with 2% FBS, 1% penicillin-streptomycin, 1% GlutaMAX and 25 mM Hepes). Viruses were passaged three times before being used for experiments. For the last passage, viruses were purified through a 20% sucrose cushion by ultracentrifugation at 80,000 x g for 2 hours at 4°C. Pellets were resuspended in HNE 1X pH7.4 (Hepes 5 mM, NaCl 150 mM, EDTA 0.1 mM), aliquoted and stored at -80°C.

Viruses titer was ascertained by plaque assays in Vero E6 cells and expressed as PFU per ml. Cells were incubated for 1 hour with 10-fold dilution of viral stocks. The inoculum was then replaced with Avicel 2.4% mixed at equal volume with DMEM supplemented with 4% FBS, 2% Glutamax, 50mM MgCl<sub>2</sub>, 0.225 % of NaHCO<sub>3</sub>, and incubated 3 days at 37°C before plaque counting.

## **Infection assays**

Vero cells were plated (50,000 cell per well) in p24-well plates 4 hours before being incubated with SARS-CoV-2 diluted in DMEM-2%. Freshly purified pDC were seeded

in p96-well plates (50,000 cells per well) and incubated with SARS-CoV-2 diluted in pDCs culture medium (RPMI 1640 Medium with GlutaMAX, 10% of FBS, 1% of MEM NEAA, 1% of Sodium Pyruvate, and 1% of Penicillin/Streptomycin). At 2, 24 and 48 hour post-inoculation, Vero cells were trypsinized and transferred to p96-well plates. Vero and pDC were washed with PBS and fixed with 2% (v/v) paraformaldehyde (PFA) diluted in PBS for 15 min at room temperature. Cells were incubated for 1 hour at 4°C with 1µg/ml of anti-nucleoprotein mAb (40143-MM05; Sino Biological) diluted in permeabilization flow cytometry buffer (PBS supplemented with 5% FBS, 0.5% (w/v) saponin, 0.1% Sodium azide). After washing, cells were incubated with 1µg/ml of Alexa Fluor 488 (115-545-003; Jackson ImmunoResearch) or 647-conjugated (115-606-062; Jackson ImmunoResearch) goat anti-mouse IgG diluted in permeabilization flow cytometry buffer for 30 min at 4°C. SARS-CoV-2 infection was quantified by flow cytometry.

To quantify infectious viral particle released in the supernatants of infected cells, pDC and Vero cells were inoculated with SARS-CoV-2 as described above and incubated at 37°C for 72-hour. At indicated time points, supernatants were collected and kept at -80°C. Virus titer were then determined by plaque assay on Vero E6 cells as described above.

### **Kinetic of infection by qPCR assay**

Vero E6 and pDC were inoculated with SARS-CoV-2 as described above. At the indicated time points, cells were washed thrice with PBS. Vero E6 were further incubated with trypsin 0.25% for 5 min at 37°C to remove cells surface bound particles. Total RNA was extracted using the RNeasy plus mini kit (Qiagen) according to manufacturer's instruction. cDNAs were generated from 80 ng total RNA by using

the Maxima First Strand Synthesis Kit following manufacturer's instruction (Thermo Fisher Scientific). Amplification products were incubated with 1 Unit of RNase H for 20 min at 37 °C, followed by 10 min at 72°C for enzyme inactivation, and diluted 10-fold in DNase/RNase free water. Real time quantitative PCR was performed using a Power Syber green PCR master Mix (Fisher Thermo Scientific) on a Light Cyclor 480 (Roche). The primers used for qPCR were: E\_Sarbeco\_F1 (5'-ACAGGTACGTTAATAGTTAATAGCGT-3'), E\_Sarbeco\_R2 (5'-ATATTGCAGCAGTACGCACACA-3') for viral RNA quantification. The plasmid containing the sequence corresponding to the amplified cDNA was purchased from GenScript (pUC57-2019-nCoV-PC:E; MC\_0101078) and serially diluted (294 to  $2.94 \times 10^9$  genes copies/μl) to generate standard curves.

### **pDC activation**

Freshly sorted pDC were cultured in p96-well plates at a concentration of  $5 \times 10^5$  cells per ml in the presence of medium alone (RPMI 1640 Medium with GlutaMAX, 10% of FBS, 1% of MEM NEAA, 1% of Sodium Pyruvate, and 1% of Penicillin/Streptomycin), influenza virus A (Charles River, A/PR/8/34, 2μg/ml), the SARS-CoV-2 primary strain 220\_95 or 211\_61 at a multiplicity of infection (MOI) of 1. After 24 or 48h of culture, pDC supernatant was collected and store at -80°C for subsequent cytokine quantification. PDC were stain for flow cytometry analysis.

### **Flow cytometry analysis**

To sort pDC, cells were stained with zombie violet or BUV fixable viability dye (Biolegend), FITC anti-CD16 (BD, clone NKP15), FITC anti-CD14 (Miltenyi, clone

TÜK4), FITC anti-CD19 (Miltenyi, clone LT19), FITC anti-CD20 (BD, clone 2H7), FITC anti-CD56 (Biolegend, clone HCD56), FITC anti-CD3 (BD, clone HIT3a), BV650 or AF700 anti-CD4 (Biolegend, clone OKT4), PE-Cy7 anti-CD11c (Biolegend, clone Bu15), APC-Vio770 anti-CD2 (Miltenyi, clone LT2), and APC anti-CD5 (BD, clone UCHT2). PDCs were gated as live, lineage<sup>-</sup> (CD16, CD14, CD19, CD20, CD56 and CD3), CD2<sup>-</sup> CD5<sup>-</sup>, and CD4<sup>+</sup> CD11c<sup>-</sup> cells.

For pDC diversification and checkpoint assessment, cells were stain with zombie violet fixable viability dye (Biolegend), BV711 anti-CD123 (Biolegend, clone 6H6), PE anti-CD80 (BD, clone L307.4), PerCP efluor 710 anti-PD-L1 (eBioscience, clone MIH1), BUV737 anti-CD86 (BD, clone 2331), BV421 anti-OX40 Ligand (BD, clone ik-1), APC anti-CD62L (BD, clone DREG-56), FITC anti-CCR7 (R&D System, clone 150503).

For ACE2 cell surface expression, indicated cells were incubated with a goat anti-human ACE2 polyclonal Ab (5 µg/ml; AF933 Biotechne) in 100 µl of PBS with 0.02% NaN<sub>3</sub> and 5% FBS for 1 h at 4°C. Cells were then washed and incubated with a Alexa 647-conjugated secondary antibody (Jackson ImmunoResearch) for 30 min at 4°C. Acquisition was performed on an Attune NxT Flow Cytometer (Thermo Fisher Scientific) or a LSR Fortessa (BD Biosciences), and analysis was done by using FlowJo software (Tree Star). Flow cytometry analysis were performed at flow cytometry core facility of IRSL (Paris, France).

### **Inflammatory cytokines measurement**

PDC cytokine production of IFN-α<sub>2</sub>, IL-8, IL-6, IP-10 and TNF-α, was measured in culture supernatants using BD cytometric bead array (CBA), according to the



manufacturer's protocol, with a 20pg/ml detection limit. Acquisitions were performed on a LSR Fortessa (BD Biosciences), and cytokine concentrations were determined using FCAP Array Software (BD Biosciences).

The concentration of secreted IFN- $\lambda$ 1 was measured by enzyme-linked immunosorbent assay (ELISA) (R&D Systems, DuoSet DY7246), according to the manufacturer's instructions. The manufacturer reported no cross-reactivity nor interference with IFN- $\alpha$ , IFN- $\beta$  1a, IL-10R $\beta$ , IFN- $\lambda$ 2 and  $\lambda$ 3, and IL-28R $\alpha$ . The optical density value (OD) of the supernatants was defined as its absolute OD value, minus the OD Absorbance from blank wells. The detection limit was 85pg/ml and all samples were run in duplicates.

## **Statistical analysis**

Statistical analyses were performed with one-way ANOVA, Kruskal Wallis's test with Dunn's multiple comparison post-test or Mann Whitney's test, in Prism (GraphPad Software).

## **Author contributions**

Ali Amara and Vassili Soumelis conceived the study. Fanny Onodi, Lucie Bonnet-Madin, Ali Amara and Vassili Soumelis designed the experiments. Fanny Onodi performed the pDC purification and FACS analysis with Justine Poirot. Lucie Bonnet-Madin and Laurent Meertens performed the virus strain isolation and the infection studies. Fanny Onodi and Léa Karpf performed cytokine quantification. Constance Delaugerre and Jérôme Legoff performed the sequencing of the SARS-CoV-2

strains. Fanny Onodi, Ali Amara and Vassili Soumelis wrote the initial manuscript draft and other authors contributed to its editing in its final form.

## **Competing interest**

The authors declare no competing interests.

## **Acknowledgments**

Ali Amara's lab received fundings from the French Government's Investissement d'Avenir program, Laboratoire d'Excellence "Integrative Biology of Emerging Infectious Diseases" (grant n°ANR-10-LABX-62-IBEID), the Fondation pour la Recherche Medicale (grant FRM - EQU202003010193), the Agence Nationale de la Recherche (ANR FLASH COVID project IDISCOVER co-founded by the Fondation pour la Recherche Médicale), University of Paris (Plan de Soutien Covid-19 : RACPL20FIR01-COVID-SOUL). Vassili Soumelis' team was supported by Agence Nationale de la Recherche (ANR-17-CE15-0003, ANR-17-CE15-0003-01), and by Université de Paris « PLAN D'URGENCE COVID19». The authors thank Maud Salmona, Severine Mercier-Delarue and Tiffanie Bouillé (Laboratoire de Virologie, Hôpital Saint Louis) for SARS-CoV-2 deep sequencing, Marie Laure Chaix (Laboratoire de Virologie, Hôpital Saint Louis) for the nasopharyngeal swabs and Lauriane Goldwirt (Laboratoire de Pharmacologie Biologique, Hôpital Saint-Louis) for providing us with hydroxychloroquine. The authors thank all the "Personnel Soignant de l'Hôpital Saint-Louis" for their amazing work during the COVID-19 epidemic. Ali Amara dedicates this work to the memory of his mentor Pr Jean-Louis Virelizier (Unité d'Immunologie Virale, Institut Pasteur, Paris), who left us during the pandemic.

## References

- Abe, M., and A.W. Thomson. 2006. Dexamethasone preferentially suppresses plasmacytoid dendritic cell differentiation and enhances their apoptotic death. *Clin. Immunol.* 118:300–306. doi:10.1016/j.clim.2005.09.019.
- Acharya, D., G. Liu, and M.U. Gack. 2020. Dysregulation of type I interferon responses in COVID-19. *Nat. Rev. Immunol.* doi:10.1038/s41577-020-0346-x.
- Alcumbre, S.G., V. Saint-André, J. Di Domizio, P. Vargas, P. Sirven, P. Bost, M. Maurin, P. Maiuri, M. Wery, M.S. Roman, L. Savey, M. Touzot, B. Terrier, D. Saadoun, C. Conrad, M. Gilliet, A. Morillon, and V. Soumelis. 2018. Diversification of human plasmacytoid predendritic cells in response to a single stimulus. *Nat. Immunol.* 19:63–75. doi:10.1038/s41590-017-0012-z.
- Arnalde, F.I., S.J. O'Day, C.G. Drake, B.A. Fox, B. Fu, W.J. Urba, V. Montesarchio, J.S. Weber, H. Wei, J.M. Wigginton, and P.A. Ascierto. 2020. The Society for Immunotherapy of Cancer perspective on regulation of interleukin-6 signaling in COVID-19-related systemic inflammatory response. *J Immunother Cancer.* 8. doi:10.1136/jitc-2020-000930.
- Blackwell, S.E., and A.M. Krieg. 2003. CpG-A-induced monocyte IFN-gamma-inducible protein-10 production is regulated by plasmacytoid dendritic cell-derived IFN- $\alpha$ . *J. Immunol.* 170:4061–4068. doi:10.4049/jimmunol.170.8.4061.
- Bontkes, H.J., J.J. Ruizendaal, D. Kramer, C.J.L.M. Meijer, and E. Hooijberg. 2005. Plasmacytoid dendritic cells are present in cervical carcinoma and become activated by human papillomavirus type 16 virus-like particles. *Gynecol. Oncol.* 96:897–901. doi:10.1016/j.ygyno.2004.10.040.
- Cervantes-Barragan, L., R. Züst, F. Weber, M. Spiegel, K.S. Lang, S. Akira, V. Thiel, and B. Ludewig. 2007. Control of coronavirus infection through plasmacytoid dendritic-cell-derived type I interferon. *Blood.* 109:1131–1137. doi:10.1182/blood-2006-05-023770.
- Das, S., S. Bhowmick, S. Tiwari, and S. Sen. 2020. An Updated Systematic Review of the Therapeutic Role of Hydroxychloroquine in Coronavirus Disease-19 (COVID-19). *Clin Drug Investig.* 40:591–601. doi:10.1007/s40261-020-00927-1.
- Dolganiuc, A., S. Chang, K. Kodys, P. Mandrekar, G. Bakis, M. Cormier, and G. Szabo. 2006. Hepatitis C virus (HCV) core protein-induced, monocyte-mediated mechanisms of reduced IFN- $\alpha$  and plasmacytoid dendritic cell loss in chronic HCV infection. *J. Immunol.* 177:6758–6768. doi:10.4049/jimmunol.177.10.6758.
- Fernández Cruz, A., B. Ruiz-Antorán, A. Muñoz Gómez, A. Sancho López, P. Mills Sánchez, G.A. Centeno Soto, S. Blanco Alonso, L. Javaloyes Garachana, A. Galán Gómez, Á. Valencia Alijo, J. Gómez Irusta, C. Payares-Herrera, I. Morras Torre, E. Sánchez Chica, L. Delgado Téllez de Cepeda, A. Callejas Díaz, A. Ramos Martínez, E. Muñoz Rubio, C. Avendaño-Solá, and Puerta de

- Hierro COVID-19 Study Group. 2020. IMPACT OF GLUCOCORTICOID TREATMENT IN SARS-COV-2 INFECTION MORTALITY: A RETROSPECTIVE CONTROLLED COHORT STUDY. *Antimicrob. Agents Chemother.* doi:10.1128/AAC.01168-20.
- Florentin, J., B. Aouar, C. Dental, C. Thumann, G. Firaguay, F. Gondois-Rey, V. Soumelis, T.F. Baumert, J.A. Nunès, D. Olive, I. Hirsch, and R. Stranska. 2012. HCV glycoprotein E2 is a novel BDCA-2 ligand and acts as an inhibitor of IFN production by plasmacytoid dendritic cells. *Blood.* 120:4544–4551. doi:10.1182/blood-2012-02-413286.
- Gilliet, M., W. Cao, and Y.-J. Liu. 2008. Plasmacytoid dendritic cells: sensing nucleic acids in viral infection and autoimmune diseases. *Nat. Rev. Immunol.* 8:594–606. doi:10.1038/nri2358.
- Guernonprez, P., J. Valladeau, L. Zitvogel, C. Théry, and S. Amigorena. 2002. Antigen presentation and T cell stimulation by dendritic cells. *Annu. Rev. Immunol.* 20:621–667. doi:10.1146/annurev.immunol.20.100301.064828.
- Hirsch, I., C. Caux, U. Hasan, N. Bendriss-Vermare, and D. Olive. 2010. Impaired Toll-like receptor 7 and 9 signaling: from chronic viral infections to cancer. *Trends Immunol.* 31:391–397. doi:10.1016/j.it.2010.07.004.
- Hoffmann, M., H. Kleine-Weber, S. Schroeder, N. Krüger, T. Herrler, S. Erichsen, T.S. Schiergens, G. Herrler, N.-H. Wu, A. Nitsche, M.A. Müller, C. Drosten, and S. Pöhlmann. 2020. SARS-CoV-2 Cell Entry Depends on ACE2 and TMPRSS2 and Is Blocked by a Clinically Proven Protease Inhibitor. *Cell.* 181:271-280.e8. doi:10.1016/j.cell.2020.02.052.
- Kuznik, A., M. Bencina, U. Svaiger, M. Jeras, B. Rozman, and R. Jerala. 2011. Mechanism of endosomal TLR inhibition by antimalarial drugs and imidazoquinolines. *J. Immunol.* 186:4794–4804. doi:10.4049/jimmunol.1000702.
- Lecuit, M. 2020. Chloroquine and COVID-19, where do we stand? *Med Mal Infect.* 50:229–230. doi:10.1016/j.medmal.2020.03.004.
- Lee, M.S., C.H. Park, Y.H. Jeong, Y.-J. Kim, and S.-J. Ha. 2013. Negative regulation of type I IFN expression by OASL1 permits chronic viral infection and CD8<sup>+</sup> T-cell exhaustion. *PLoS Pathog.* 9:e1003478. doi:10.1371/journal.ppat.1003478.
- Liu, Y.-J. 2005. IPC: professional type 1 interferon-producing cells and plasmacytoid dendritic cell precursors. *Annu. Rev. Immunol.* 23:275–306. doi:10.1146/annurev.immunol.23.021704.115633.
- Mahévas, M., V.-T. Tran, M. Roumier, A. Chabrol, R. Paule, C. Guillaud, E. Fois, R. Lepeule, T.-A. Szwebel, F.-X. Lescure, F. Schlemmer, M. Matignon, M. Khellaf, E. Crickx, B. Terrier, C. Morbieu, P. Legendre, J. Dang, Y. Schoindre, J.-M. Pawlotsky, M. Michel, E. Perrodeau, N. Carlier, N. Roche, V. de Lastours, C. Ourghanlian, S. Kerneis, P. Ménager, L. Mouthon, E. Audureau, P. Ravaud, B. Godeau, S. Gallien, and N. Costedoat-Chalumeau. 2020. Clinical efficacy of hydroxychloroquine in patients with covid-19 pneumonia

- who require oxygen: observational comparative study using routine care data. *BMJ*. 369:m1844. doi:10.1136/bmj.m1844.
- Marsili, G., A.L. Remoli, M. Sgarbanti, E. Perrotti, A. Fragale, and A. Battistini. 2012. HIV-1, interferon and the interferon regulatory factor system: an interplay between induction, antiviral responses and viral evasion. *Cytokine Growth Factor Rev*. 23:255–270. doi:10.1016/j.cytogfr.2012.06.001.
- Meera, S., T. Madhuri, G. Manisha, and P. Ramesh. 2010. Irreversible loss of pDCs by apoptosis during early HIV infection may be a critical determinant of immune dysfunction. *Viral Immunol*. 23:241–249. doi:10.1089/vim.2009.0112.
- Meyers, J.H., J.S. Justement, C.W. Hallahan, E.T. Blair, Y.A. Sun, M.A. O’Shea, G. Roby, S. Kottlil, S. Moir, C.M. Kovacs, T.-W. Chun, and A.S. Fauci. 2007. Impact of HIV on Cell Survival and Antiviral Activity of Plasmacytoid Dendritic Cells. *PLoS ONE*. 2:e458. doi:10.1371/journal.pone.0000458.
- Nandakumar, K. 2020. COVID-19: Emergence, Spread, Possible Treatments, and Global Burden. *Frontiers in Public Health*. 8:13.
- Pons, S., S. Fodil, E. Azoulay, and L. Zafrani. 2020. The vascular endothelium: the cornerstone of organ dysfunction in severe SARS-CoV-2 infection. *Crit Care*. 24:353. doi:10.1186/s13054-020-03062-7.
- Sacre, K., L.A. Criswell, and J.M. McCune. 2012. Hydroxychloroquine is associated with impaired interferon- $\alpha$  and tumor necrosis factor- $\alpha$  production by plasmacytoid dendritic cells in systemic lupus erythematosus. *Arthritis Res. Ther*. 14:R155. doi:10.1186/ar3895.
- Scheuplein, V.A., J. Seifried, A.H. Malczyk, L. Miller, L. Höcker, J. Vergara-Alert, O. Dolnik, F. Zielecki, B. Becker, I. Spreitzer, R. König, S. Becker, Z. Waibler, and M.D. Mühlebach. 2015. High secretion of interferons by human plasmacytoid dendritic cells upon recognition of Middle East respiratory syndrome coronavirus. *J. Virol*. 89:3859–3869. doi:10.1128/JVI.03607-14.
- Sheahan, T.P., and M.B. Frieman. 2020. The continued epidemic threat of SARS-CoV-2 and implications for the future of global public health. *Curr Opin Virol*. 40:37–40. doi:10.1016/j.coviro.2020.05.010.
- Snell, L.M., T.L. McGaha, and D.G. Brooks. 2017. Type I Interferon in Chronic Virus Infection and Cancer. *Trends Immunol*. 38:542–557. doi:10.1016/j.it.2017.05.005.
- Soumelis, V., I. Scott, F. Gheyas, D. Bouhour, G. Cozon, L. Cotte, L. Huang, J.A. Levy, and Y.J. Liu. 2001. Depletion of circulating natural type 1 interferon-producing cells in HIV-infected AIDS patients. *Blood*. 98:906–912. doi:10.1182/blood.v98.4.906.
- Tang, D., P. Comish, and R. Kang. 2020. The hallmarks of COVID-19 disease. *PLoS Pathog*. 16:e1008536. doi:10.1371/journal.ppat.1008536.

- Tay, M.Z., C.M. Poh, L. Rénia, P.A. MacAry, and L.F.P. Ng. 2020. The trinity of COVID-19: immunity, inflammation and intervention. *Nat. Rev. Immunol.* 20:363–374. doi:10.1038/s41577-020-0311-8.
- Thomas, J.M., Z. Pos, J. Reinboth, R.Y. Wang, E. Wang, G.M. Frank, P. Lusso, G. Trinchieri, H.J. Alter, F.M. Marincola, and E. Thomas. 2014. Differential Responses of Plasmacytoid Dendritic Cells to Influenza Virus and Distinct Viral Pathogens. *Journal of Virology.* 88:10758–10766. doi:10.1128/JVI.01501-14.
- Touret, F., and X. de Lamballerie. 2020. Of chloroquine and COVID-19. *Antiviral Res.* 177:104762. doi:10.1016/j.antiviral.2020.104762.
- Vabret, N., G.J. Britton, C. Gruber, S. Hegde, J. Kim, M. Kuksin, R. Levantovsky, L. Malle, A. Moreira, M.D. Park, L. Pia, E. Risson, M. Saffern, B. Salomé, M. Esai Selvan, M.P. Spindler, J. Tan, V. van der Heide, J.K. Gregory, K. Alexandropoulos, N. Bhardwaj, B.D. Brown, B. Greenbaum, Z.H. Gümüş, D. Homann, A. Horowitz, A.O. Kamphorst, M.A. Curotto de Lafaille, S. Mehandru, M. Merad, R.M. Samstein, and Sinai Immunology Review Project. 2020. Immunology of COVID-19: Current State of the Science. *Immunity.* 52:910–941. doi:10.1016/j.immuni.2020.05.002.
- Villani, A.-C., R. Satija, G. Reynolds, S. Sarkizova, K. Shekhar, J. Fletcher, M. Griesbeck, A. Butler, S. Zheng, S. Lazo, L. Jardine, D. Dixon, E. Stephenson, E. Nilsson, I. Grundberg, D. McDonald, A. Filby, W. Li, P.L. De Jager, O. Rozenblatt-Rosen, A.A. Lane, M. Haniffa, A. Regev, and N. Hacohen. 2017. Single-cell RNA-seq reveals new types of human blood dendritic cells, monocytes, and progenitors. *Science.* 356. doi:10.1126/science.aah4573.
- Wang, M., R. Cao, L. Zhang, X. Yang, J. Liu, M. Xu, Z. Shi, Z. Hu, W. Zhong, and G. Xiao. 2020. Remdesivir and chloroquine effectively inhibit the recently emerged novel coronavirus (2019-nCoV) in vitro. *Cell Res.* 30:269–271. doi:10.1038/s41422-020-0282-0.
- Wilk, A.J., A. Rustagi, N.Q. Zhao, J. Roque, G.J. Martínez-Colón, J.L. McKechnie, G.T. Ivison, T. Ranganath, R. Vergara, T. Hollis, L.J. Simpson, P. Grant, A. Subramanian, A.J. Rogers, and C.A. Blish. 2020. A single-cell atlas of the peripheral immune response in patients with severe COVID-19. *Nature Medicine.* 1–7. doi:10.1038/s41591-020-0944-y.
- Yang, C.-W., T.-T. Peng, H.-Y. Hsu, Y.-Z. Lee, S.-H. Wu, W.-H. Lin, Y.-Y. Ke, T.-A. Hsu, T.-K. Yeh, W.-Z. Huang, J.-H. Lin, H.-K. Sytwu, C.-T. Chen, and S.-J. Lee. 2020. Repurposing old drugs as antiviral agents for coronaviruses. *Biomed J.* doi:10.1016/j.bj.2020.05.003.
- Yin, Z., J. Dai, J. Deng, F. Sheikh, M. Natalia, T. Shih, A. Lewis-Antes, S.B. Amrute, U. Garrigues, S. Doyle, R.P. Donnelly, S.V. Kotenko, and P. Fitzgerald-Bocarsly. 2012. Type III IFNs are produced by and stimulate human plasmacytoid dendritic cells. *J. Immunol.* 189:2735–2745. doi:10.4049/jimmunol.1102038.



## Figure legends

Figure 1. **SARS-CoV-2 induces activation and diversification of primary human pDC.** Sorted blood pDC from healthy donors were cultured for 24h with either Medium, SARS-CoV-2, or Influenza virus A (Flu). **(A)** Dotplot showing pDC activation and diversification through the expression of PD-L1 and CD80 into P1-, P2-, and P3-subpopulations. **(B)** Quantification of the three populations. Bars represent medians of n=5 healthy donors. \*P < 0.05; \*\*P < 0.01; Mann Whitney test. **(C)** Dotplot showing pDC activation from different strains of SARS-CoV-2 isolated from two patients. **(D)** Percentage of live pDC after 24h of culture with either Medium, SARS-CoV-2, or Influenza virus A (Flu). **(E)** Histogram of ACE2-expression on pDC, Vero E6 and 293T-ACE2 (black) compared to the isotype (light grey). **(F)** Intracellular production of SARS-CoV-2 Ribonucleoprotein in Vero E6 and pDC at 2, 24 or 48h post infection (hpi) with SARS-CoV-2. **(G)** Infectious viral titers in the supernatants of SARS-CoV-2-infected Vero E6 and pDC at 2, 24, 48 or 72h post infection (hpi).

Figure 2. **SARS-CoV-2 induces pDC activation in a dose dependent manner.** Sorted blood pDC from healthy donors were cultured for 24h with either Medium, Influenza virus A (Flu), or SARS-CoV-2 at a MOI of 0.04, 0.2, or 1. **(A)** Dotplot showing pDC activation through the expression of PD-L1 and CD80. **(B)** Quantification of the three populations. Bars represent medians of n=3 healthy donors. \*P < 0.05; ns: not significant; Mann Whitney test. **(C)** PDC geometric mean (MFI) of activation markers after 24h of culture with either Medium, Influenza virus A, or SARS-CoV-2 at a MOI of 1. Histograms represent medians and bars interquartile

of n=5 healthy donors. \*P < 0.05; \*\*P < 0.01; \*\*\*P < 0.001; Kruskal-Wallis with Dunn's multiple comparison's post test.

### Figure 3. **SARS-CoV-2-activated pDC produce pro-inflammatory cytokines.**

Sorted blood pDC from healthy donors were cultured for 24h or 48h with either Medium, Influenza virus A (Flu), or SARS-CoV-2 at a MOI of 1. **(A)** Quantification of pro-inflammatory cytokines at 24h. Bars represent medians of n=5 healthy donors. **(B)** Quantification of pro-inflammatory cytokines at 48h. Bars represent medians of n=3 healthy donors. \*P < 0.05; \*\*P < 0.01; ns: not significant; Mann Whitney test.

### Figure 4. **SARS-CoV-2-induced pDC activation is inhibited by hydroxychloroquine.**

Sorted blood pDC from healthy donors were cultured for 24h with either Medium, Influenza virus A (Flu), or SARS-CoV-2 at a MOI 1 with or without the presence of hydroxychloroquine (HCQ). **(A)** Dotplot showing pDC diversification in P1-, P2-, and P3-subpopulations in the presence of HCQ. **(B)** Quantification of the three populations. **(C)** Histograms of pDC's activation markers. **(D)** Geometric mean (MFI) of activation markers. Histograms represent medians and bars interquartile of n=3 healthy donors. **(E)** Quantification of pro-inflammatory cytokines production. Bars represent medians of n=3 healthy donors. \*P < 0.05; ns: not significant; Mann Whitney test.

### Figure S1. **SARS-CoV-2 induces pDC activation.**

Sorted blood pDC from healthy donors were cultured for 24h with either Medium, SARS-CoV-2, or Influenza virus A (Flu). **(A)** Pourcentage of pure pDC among live cells through different sorting strategies. **(B)** P1-, P2- and P3- diversification of fresh, fluorescent sorted pDC



versus frozen, magnetic sorted pDC with either SARS-CoV-2 or Influenza virus A (Flu) for 24h. **(C)** Dotplot of pDC activation with either free SARS-CoV-2 or pDC co-culture with SARS-CoV-2 infected cells. **(D)** Viral RNA copy number in of Vero E6 and pDC 2, 24 and 48h post infection (hpi). **(E)** Intracellular production of the nucleoprotein antigen (N) on pDC of two healthy donors.

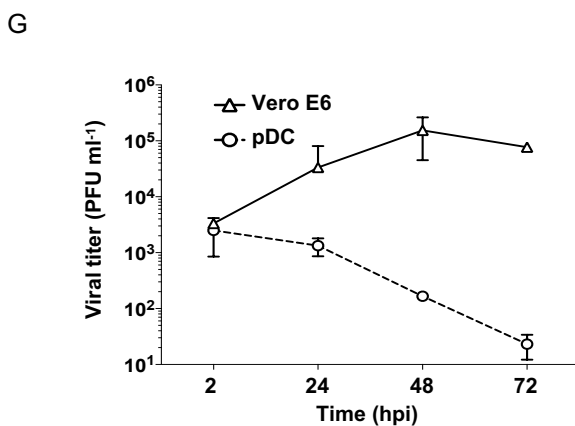
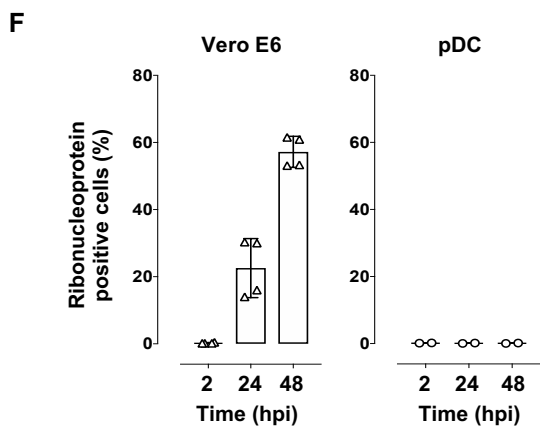
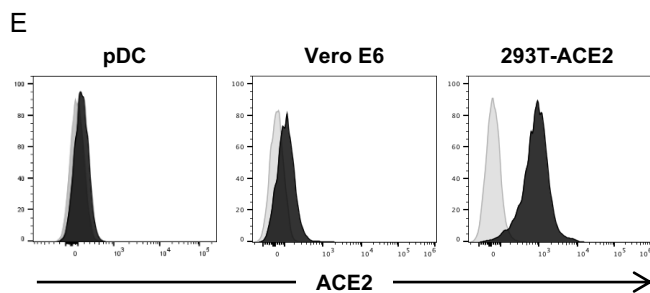
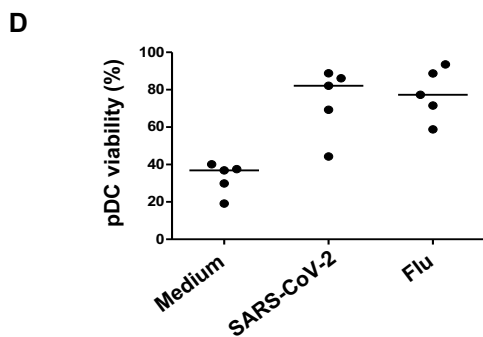
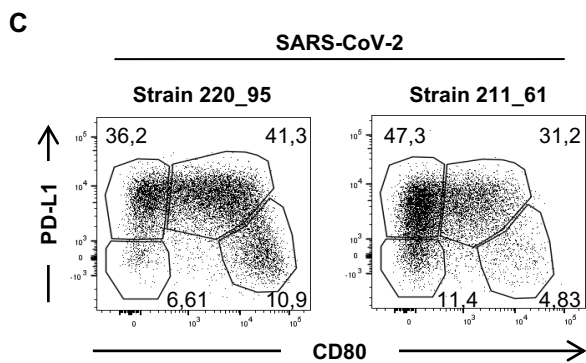
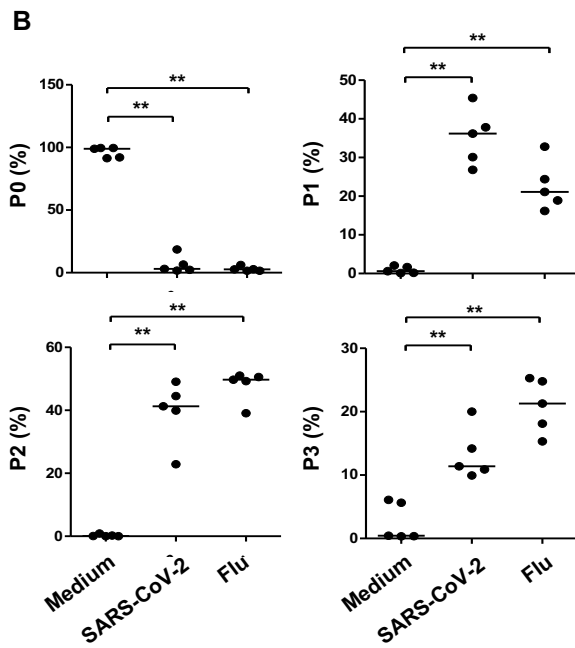
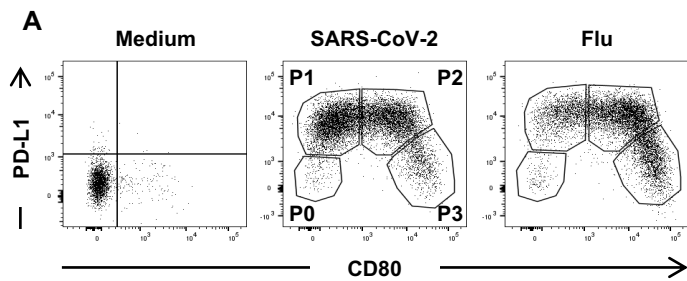
**Figure S2. SARS-CoV-2 induces activation and diversification of tonsilar pDCs.**

Sorted blood pDC from healthy donors were cultured for 48h with either Medium, SARS-CoV-2, or Influenza virus A (Flu). **(A)** Dotplot showing pDC activation and diversification through the expression of PD-L1 and CD80 at 24h and 48h. **(B)** Geometric mean (MFI) of pDC's activation markers at 48h. Histograms represent medians and bars interquartils of n=3 healthy donors. \*P < 0.05; Kruskal-Wallis with Dunn's multiple comparison's post test. **(C)** Dotplot of tonsil pDC activation cultured for 24h with either Medium, SARS-CoV-2 or Influenza virus A (Flu). **(D)** Quantification of pro-inflammatory cytokines of tonsilar pDC at 24h. Histograms represent medians of n=1 healthy donors.

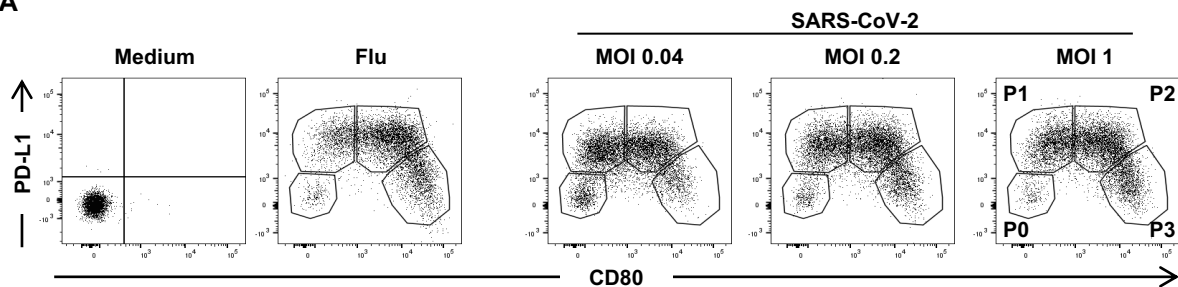
**Figure S3. Hydroxychloroquine inhibits SARS-CoV-2-induced pDC activation in a dose dependant manner.**

Sorted blood pDC from healthy donors were cultured for 24h with either Medium, Influenza virus A (Flu), or SARS-CoV-2 at a MOI 1 with hydroxychloroquine (HCQ) or vehicle. **(A)** Dotplot of pDC diversification with increasing concentration of hydroxychloroquine (HCQ) or vehicle. **(B)** Dotplot showing OX40L and CD86 in presence or absence of HCQ. **(C)** Pourcentage of OX40L<sup>high</sup> population among pDC. Bars represent medians of n=3 healthy donors.

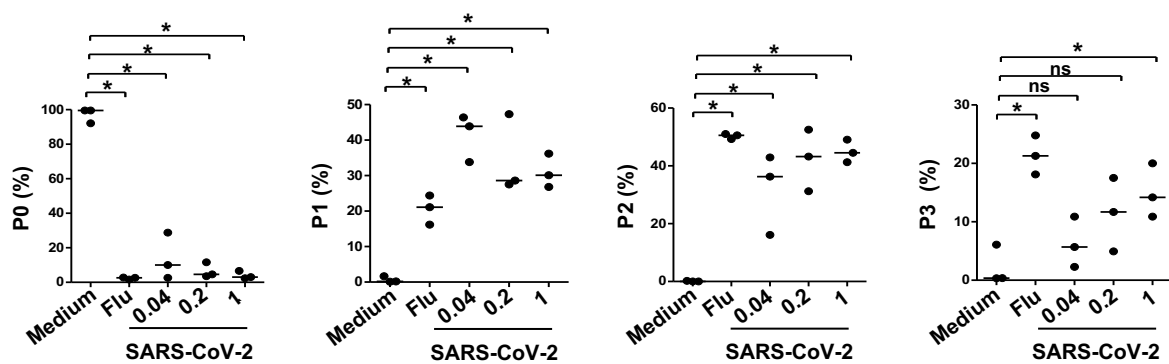
\*P < 0.05; Mann Witney test.



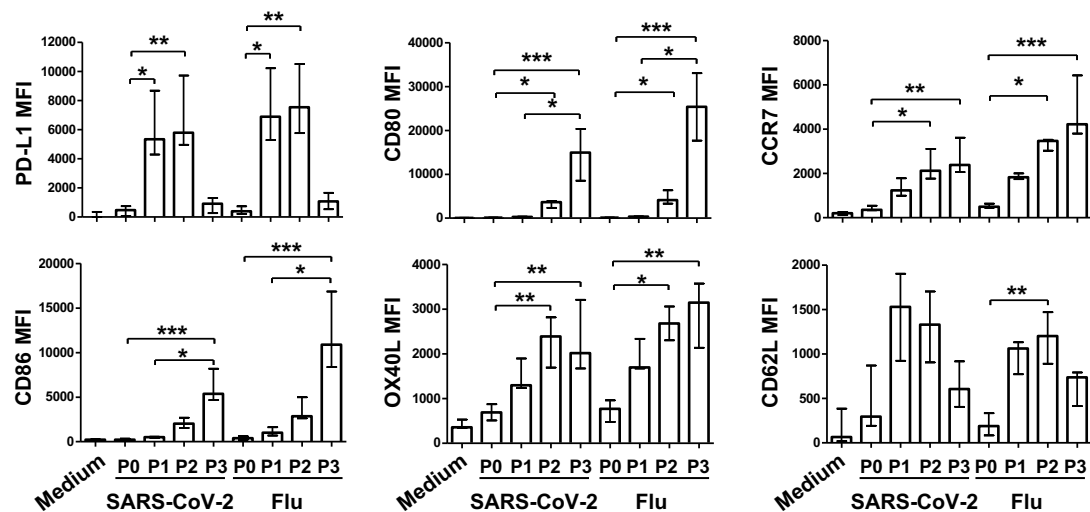
A

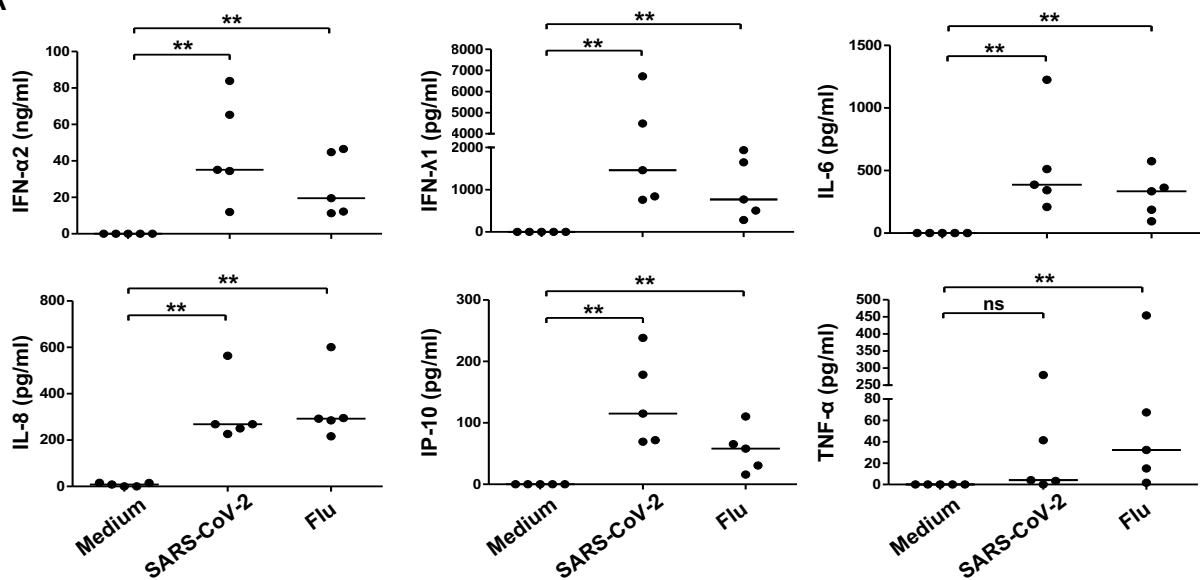


B



C



**A****B**